Vol. 636: 123–137, 2020
https://doi.org/10.3354/meps13216

MARINE ECOLOGY PROGRESS SERIES
Mar Ecol Prog Ser

Published February 20

Fine-scale horizontal distributions of multiple species of larval tuna off the Nansei Islands, Japan

Atsushi Tawa[1,*], Taketoshi Kodama[2], Kay Sakuma[2], Taiki Ishihara[1], Seiji Ohshimo[1,3]

[1]National Research Institute of Far Seas Fisheries, 5-7-1 Orido Shimizu-ku, Shizuoka City, Shizuoka 424-8633, Japan
[2]Japan Sea National Fisheries Research Institute, 1-5939-22, Suido, Chuou-ku, Niigata City, Niigata 951-8121, Japan
[3]Seikai National Fisheries Research Institute, 1551-8, Taira, Nagasaki City, Nagasaki 851-2213, Japan

ABSTRACT: To quantitatively evaluate the distribution of tuna larvae relative to oceanographic conditions, we conducted investigations off the Nansei Islands in the western North Pacific in June from 2015 to 2017. Five species, namely Pacific bluefin tuna *Thunnus orientalis* (PBF), yellowfin tuna *T. albacares* (YFT), skipjack tuna *Katsuwonus pelamis* (SKJ), frigate tuna *Auxis thazard*, and bullet tuna *A. rochei* (BT), were collected in each year. The most dominant species was BT throughout the 3 yr period, followed by SKJ in 2015 and YFT in 2016 and 2017. The horizontal larval distributions of the 5 species were largely influenced by the Kuroshio Current: larvae of the 2 *Auxis* species were distributed in the Kuroshio and the Kuroshio inshore waters, whereas those of the other species were found in the Kuroshio offshore waters. These differences are consistent with the differences in spawner distributions among the tunas. Generalized additive models (GAMs) indicated that the larval densities were affected by the sea surface height anomaly and that the larvae were not always amassed by horizontal transport. Sea surface temperature (SST) and salinity possibly influenced the larval physiology and survival, thereby determining their densities. In the GAMs, PBF and YFT showed similar responses to SST, and YFT and SKJ similarly responded to salinity. To avoid overlapping their ecological niches, the larvae of 3 species (PBF, YFT, and SKJ) are expected to differ in other ways, including their vertical distributions and feeding habits.

KEY WORDS: Competitive exclusion principle · Generalized additive model · Scombridae · Larval distribution · Interspecific interaction

1. INTRODUCTION

Tunas, which are medium- to large-sized fish belonging to the tribe Thunnini, are of high economic value (Collette et al. 2011), and the total catch of tunas in the world's oceans has nearly doubled over the past 30 yr (Majkowski 2007). However, several tuna populations are experiencing decreased or historically low levels, and their conservation and management are global concerns (Collette et al. 2011).

To properly manage resources, it is important to understand that recruitment varies according to the survival of the larval phase as well as the juvenile phase (Leggett & Deblois 1994). Habitats, such as physical environments and feeding environments, during the larval period generally determine larval growth, survival, and ultimately recruitment (Houde 1997); this 'growth-dependent survival' hypothesis can be adopted for tunas. Although growth-dependent survival is still unclear in tuna species other than Pacific bluefin tuna *Thunnus orientalis* (PBF), otolith analysis has indicated that only rapidly growing PBF larvae can survive and become juveniles, and selection mainly occurs in the 5–10 mm body length range (Tanaka et al. 2006, Satoh et al. 2013, Watai et al. 2017, 2018, Ishihara et al. 2019). The ability to feed on prey in the water and feeding rate have been associated with larval growth of bluefin tunas (Jenkins et al. 1991, Satoh et al. 2013), and water temperature also has an effect (Ishihara et al. 2019). Not only the biological environments but also the physical oceanographic conditions determine larval tuna distributions.

*Corresponding author: atawa2015@affrc.go.jp

For example, Ohshimo et al. (2017) evaluated the habitat conditions of PBF larvae based on a generalized additive model (GAM) and suggested that the optimal sea surface temperature (SST) for this species ranges from 24 to 29°C. Reglero et al. (2014) reported that the horizontal habitats of tuna larvae are associated with water temperature and eddy kinetic energy.

The effects of multiple species interactions also need to be considered, given that the horizontal distributions of larval tunas overlap globally (Nishikawa et al. 1985). Gause's competitive exclusion principle (Hardin 1960), which states that only a single species can survive when the ecological niches of multiple species overlap, has been applied to fishes. To avoid overlapping ecological niches, the feeding habits of co-occurring larval tunas (Llopiz & Hobday 2015), as well as their vertical distributions, differ among species (Habtes et al. 2014). In addition, the fine-scale horizontal distributions of larval tunas may also differ. For example, the horizontal distributions of larval tunas are associated with meso-scale eddies and physio-chemical environments in the northern part of the Gulf of Mexico (Cornic et al. 2018): Atlantic bluefin tuna *T. thynnus* inhabit cold-core eddies and saline waters, while blackfin tuna *T. atlanticus*, bigeye tuna *T. obesus*, and yellowfin tuna *T. albacares* (YFT) inhabit warm-water eddies and both saline and less-saline waters (Cornic et al. 2018).

The offshore area of the Nansei Islands, Japan, where the Kuroshio Current flows along the continental shelf edge (Fig. 1a), is a spawning and nursery area for multiple species of tunas including PBF, YFT, and skipjack tuna *Katsuwonus pelamis* (SKJ) (Nishikawa et al. 1985, Ashida et al. 2015, Okochi et al. 2016). This area is important for PBF recruitment because there are only 3 known PBF spawning fields in the world (Ohshimo et al. 2018a,b, Tanaka et al. 2020), and the variation in SST of this area in June significantly explains the variations in the PBF stock (Nakayama et al. 2019). On the continental shelf of the East China Sea adjacent to the Nansei Islands and the Kuroshio, egg and larval fish assemblages have been seasonally reported in previous studies (Sassa & Konishi 2015, Lin et al. 2016). Larvae of small pelagic fishes, such as mackerels (*Scomber* spp.), Japanese jack mackerel *Trachurus japonicus*, and lantern fish *Myctophum asperum* have been observed in winter, and their distribution patterns have been classified into 3 categories: the Kuroshio, continental shelf-break, and continental shelf assemblages (Sassa & Konishi 2015). SST and chlorophyll (chl) *a* concentrations have been used to characterize the larval distributions both in winter and summer in this area (Sassa & Konishi 2015, Lin et al. 2016). In contrast, little is known about the larval fish assemblages upstream of the Kuroshio and the Kuroshio offshore waters. The oceanic environments are homogeneous in the surface mixed layer during summer (Kodama et al. 2011, 2015) and contain the lowest primary productivity in the larval tuna nursery

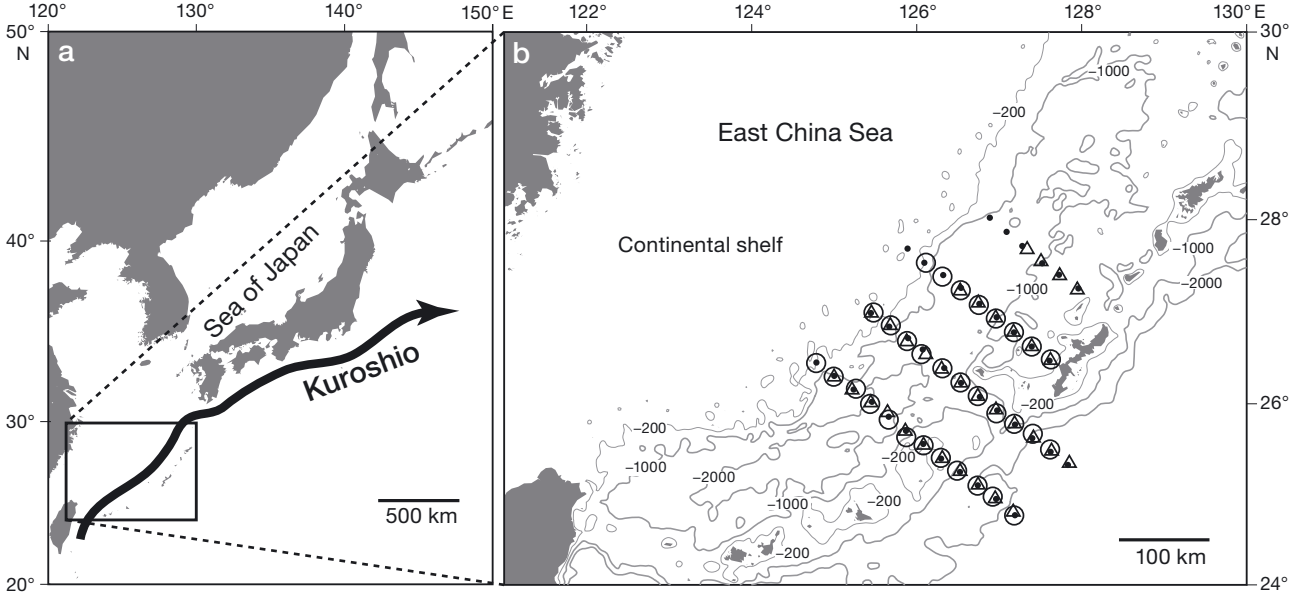

Fig. 1. (a) Sampling region in the western North Pacific, indicating the location of the Nansei Islands (rectangle). The black line and arrow indicates the position and direction of the Kuroshio Current. (b) Continental shelf located northwest of the 200 m depth contour, as well as the 1000 and 2000 m depth contours. Symbols show the stations sampled during the 2015 (●), 2016 (△), and 2017 (○) cruises, respectively

grounds (Llopiz & Hobday 2015). In comparison to the Kuroshio inshore waters, the Kuroshio offshore waters are regarded as homogeneous; whether larval tuna distributions are segregated or overlap needs to be determined. Investigations of larval tuna assemblies in this area are expected to provide us with a better understanding of larval tuna habitats and the associated oceanographic factors; however, previous studies in this area (Suzuki et al. 2014, Ohshimo et al. 2017) only focused on PBF larvae, and the presence of larvae of other tuna species was not investigated.

In this study, we conducted fine-scale larval surveys, including surveys of the continental shelf edge and offshore waters of the Nansei Islands, where multiple species of tuna larvae are present, and examined the correlations between the horizontal distribution patterns of tuna larvae and environmental factors. We evaluated the horizontal habitats of multiple species of tuna larvae off the Nansei Islands and identified the environmental factors that significantly influenced the tuna distributions.

2. MATERIALS AND METHODS

2.1. Observations

Field observations were conducted during 3 cruises of the RV 'Shunyo-Maru' (Japan Fisheries Research and Education Agency) during 14–30 June 2015, 14–30 June 2016, and 16–28 June 2017; June is the spawning season of PBF, which was the main target species of these investigations. We sampled 39, 33, and 30 stations in 2015, 2016, and 2017, respectively, in the offshore waters of the Nansei Islands (Fig. 1b). The bottom depths (BDs) ranged from 124 to 3319 m. The vertical profiles of salinity, temperature, and chl *a* fluorescence were measured at all sampling sites using a conductivity, temperature, and depth sensor (SBE 9plus, Seabird Electronics) with a fluorometer (Seapoint). The fluorescence data of discrete measurements collected in the 10–200 m depth layers were converted to chl *a* concentrations using the method of Welschmeyer (1994). SST was measured with a calibrated mercury thermometer using a bucket, and the sea surface salinity of the water collected with the bucket was measured by an Autosal salinometer (8400B, Guildline Instruments).

The total density of zooplankton was evaluated from samples collected by a vertical tow of a long North Pacific standard (NORPAC) net (net mouth diameter: 0.45 m, mesh size: 0.1 mm; 13XX, RIGO) from 200 m depth to the surface. The surveys with the NORPAC net were conducted at night, from 19:00 to 04:00 h. The volume of water filtered by the NORPAC net was estimated with a mechanical flowmeter (RIGO) installed at the mouth of the net. When BD was <210 m, the tow was 10 m above the bottom. The samples were fixed with neutral formalin soon after collection, and their abundance, including the abundance of non-arthropod zooplankton such as appendicularians, was estimated based on the density of individuals in these samples. We collected zooplankton from 20 m depth to the surface using the same gear used to collect zooplankton from 200 m depth during the 2016 cruise. In a comparison of the logarithmic transformations of zooplankton densities from 200 to 20 m, a significant positive correlation was observed (r^2 = 0.19, n = 33); thus, we considered zooplankton densities from 200 m to the surface to be an index of the surface zooplankton densities.

The northern and southern boundaries of the Kuroshio area were defined based on the Quick Bulletin of Ocean Conditions issued by the Japan Coast Guard (www1.kaiho.mlit.go.jp/KANKYO/KAIYO/qboc/index_E.html). In the bulletin, the northern edge of the Kuroshio is generally defined by surface currents (>2 knots), SST, and sea surface height, and the southern edge is defined as 40 nautical miles (n miles) away from the northern edge. The observed area was respectively named 'Kuroshio inshore waters' for areas north of the northern boundaries of the Kuroshio, 'Kuroshio offshore waters' for areas south of the southern boundaries of the Kuroshio, and 'Kuroshio' for areas between the northern and southern boundaries of the Kuroshio. The Kuroshio axis is set in the bulletin as 13 n miles away from the northern edge, and its position was confirmed based on the temperature at 200 m during our study (16.5°C: Kawai 1969). For the identification of meso-scale eddies, we used sea surface height anomaly (SSHA) data generated every day from merged satellite altimetry measurements using Jason-1, ENVISAT/ERS, Geosat Follow-On, and Topex/Poseidon interlaced (www.aviso.altimetry.fr/en/home.html). The spatial resolution of SSHA was 0.25° by 0.25°, and the SSHA values were obtained by bilinear interpolation from the surrounding 4 grid values.

2.2. Larval identification and morphometry

Tuna larvae were collected with a 2 m diameter ring net (0.334 mm mesh and 4 m long). The net was placed on the lateral side of the ship for 10 min with a ship speed of ca. 1.5–2.0 knots. The top of the net

was set at the sea surface; the samples were collected at a depth of approximately 2 m. A flowmeter (RIGO) was installed at the mouth of the net, and filtered volumes were estimated using the flowmeter. All surveys were conducted at night, from 19:00 to 04:00 h. Tuna larvae were sorted on ice and individually cryopreserved at −30°C onboard the ship; the remnant plankton sample after sorting was fixed in ethanol and re-sorted in the laboratory. Some of the cryopreserved larvae were placed in 99.5% ethanol, whereas the others were not.

The tuna larvae were identified by a combination of morphological and genetic methods. The larvae were separated into PBF, YFT, SKJ, *Auxis* spp., and 'others', which included larvae that could not be identified (i.e. too small and not intact) based on the melanophore patterns appearing on their heads and bodies (Okiyama 2014). The identification of tuna larvae was further confirmed by several molecular techniques. Two allele-specific PCR assays were used for molecular screening of the 3 dominant species, PBF (Suzuki et al. 2014), and the 2 *Auxis* species (see the Supplement at www.int-res.com/articles/suppl/m636p123_supp.pdf). Specimens not identified in the first and second rounds were subsequently used for a sequencing analysis of the flanking region between the ATPase and CO3 genes (ATCO, Chow et al. 2003) and were submitted to a basic local alignment search tool (BLAST) search (https://blast.ncbi.nlm.nih.gov). At 10 of the stations where >100 individual *Auxis* larvae were sampled, the genetic identification of *Auxis* larvae was applied to ≥10% of the individuals, and the numbers of bullet tuna *A. rochei* (BT) and frigate tuna *A. thazard* (FT) were calculated from the ratio of the 2 species. At one station where 2465 individuals of larval *Auxis* were collected in the 2016 cruise, the genetic identification was applied to only 50 individuals (2% of the total). The notochord length (NL) or standard length (SL) of intact, DNA-identified larvae was measured using photographs taken under a light microscope. NL was measured to the nearest 0.1 mm in cases where the caudal skeleton was not well developed; SL was measured for the other specimens. The body length (NL or SL) of ethanol-fixed specimens was corrected to the original condition before fixation based on procedures outlined by Tanaka et al. (2006).

2.3. Statistical analysis

To evaluate the environmental factors used for predicting the abundance of tuna larvae, we applied a GAM with negative binomial errors. The negative binomial GAM for the catch number of each species was fitted using the 'mgcv' package (Wood 2017) in R (R Core Team 2018), with the following equations:

$$CN_i \sim NB(\mu_i, k) \quad (1)$$

$$E(CN_i) = \mu_i \quad (2)$$

$$Var(CN_i) = \mu_i + \mu_i^2/k \quad (3)$$

$$\mu_i = \exp(\alpha + f_1X_1 + f_2X_2 + \ldots + f_nX_n) \quad (4)$$

where CN_i, NB, E, Var, μ, and k represent the collected number of species i, negative binomial distribution, expected value, variance, mean, and dispersion parameter, respectively. f_nX_n represents a smoothing function of the explanatory variable. The explanatory variables in the full model were SST, chl *a* concentration at 10 m depth (Chl10), salinity at 10 m depth (S10), number of zooplankton ind. m^{-3} (Zoo), BD, distance from the northern edge of the Kuroshio (Dist), SSHA, year (Year), and volume of water filtered (Vol). The upper limitations on the degrees of freedom for every smoothing term (k) were set to 4 to avoid a biologically impossible response. Sampling years were included as factors in the model to account for interannual variation in the number of each species of tuna larvae. To correct for the amount of survey effort, the volume of filtered water was log-transformed with the natural logarithm using the method of Reglero et al. (2018). The maximum variance inflation factor of these parameters was <3. The temperature at 10 m depth and sea surface salinity were not included because of high multicollinearity and a lack of data at some stations. The difference between the sea surface salinity and salinity at 10 m depth (n = 30) was <0.3, and this difference was mostly <0.01 during the 2017 cruise. Thus, we consider the salinity at 10 m depth to be very similar to salinity at the surface. The explanatory variables and final model descriptions were selected on the basis of Akaike's information criterion (AIC) values. In 3 cases, the volume was not selected in the best model, but to treat the larval numbers in terms of larval density, the model with the lowest AIC value that contained volume was selected. The AIC values of the best model for PBF, YFT, and SKJ were 509.9, 641.1, and 533.4, respectively, but the AIC values of the final model including the volume were 510.8, 644.4, and 534.9, respectively (Table 1). In these cases, the difference in AIC values was <3.4 between the models that did or did not contain the volume.

A principal coordinate analysis (PCoA; Gower 1967), which is a multivariate analysis with Bray Curtis distances, was used to evaluate the similarity in species composition between stations. PCoA can be

Table 1. Explanatory variables selected by the final generalized additive models for 5 tuna species. Akaike's information criterion (AIC) and percent deviance explained (DE) are given for each final model. SST: sea surface temperature (°C); Chl10: chl *a* concentration at a 10 m depth (µg l^{-1}); S10: salinity at a 10 m depth; Zoo: zooplankton density (ind. m^{-3}); BD: bottom depth (m); Dist: distance from the northern edge of the Kuroshio (n miles); SSHA: sea surface height anomaly (m); Vol: volume of water filtered (m^3); PBF: Pacific bluefin tuna; YFT: yellowfin tuna; SKJ: skipjack tuna; FT: frigate tuna; BT: bullet tuna. Dashes indicate explanatory variables that were not selected in the final model. s(): smoothing function

	PBF Final model	YFT Final model	SKJ Final model	FT Final model	BT Final model
Variables					
Year	factor(Year)	factor(Year)	factor(Year)	–	factor(Year)
SST	s(SST)	s(SST)	–	–	–
Chl10	–	–	–	–	–
S10	–	s(S10)	s(S10)	–	s(S10)
Zoo	–	–	–	–	s(Zoo)
BD	–	s(BD)	s(BD)	–	–
Dist	s(Dist)	-	s(Dist)	s(Dist)	s(Dist)
SSHA	s(SSHA)	s(SSHA)	s(SSHA)	s(SSHA)	s(SSHA)
Vol	offset(log(Vol))	offset(log(Vol))	offset(log(Vol))	offset(log(Vol))	offset(log(Vol))
AIC	510.8	644.4	534.9	439.7	561.0
DE(%)	51.5	40.6	53.3	10.4	76.7

applied to data sets that contain many zeros (Legendre & Legendre 2012) and was performed using the 'vegan' package (Oksanen et al. 2019) in R (R Core Team 2018).

3. RESULTS

3.1. Environmental conditions

The horizontal distributions of the oceanographic conditions were characterized by the Kuroshio, which flowed along the continental shelf edge and the northern edge of our investigated areas during all 3 cruises. SST ranged from 26.3–29.5°C (Fig. 2): 28.4 ± 0.6°C (mean ± SD) in 2015, 28.8 ± 0.4°C in 2016, and 27.7 ± 0.7°C in 2017. In addition to temperature, the salinity at a depth of 10 m was lower on the coastal side than the offshore side, ranging from 33.81 to 34.90. The chl *a* concentration at 10 m depth varied from 0.054 to 0.314 µg l^{-1}; the mean values of chl *a* were ~0.1 µg l^{-1} in 2015 (0.095 ± 0.037 µg l^{-1}) and 2016 (0.093 ± 0.015 µg l^{-1}), but in 2017, chl *a* was always >0.1 µg l^{-1} (0.147 ± 0.048 µg l^{-1}). Zooplankton density ranged from 29.6–9037 ind. m^{-3}. The lowest value, which was observed at 25.55° N, 126.08° E in 2017, is questionable because the second lowest value (568.9 ind. m^{-3}) was approximately 20 times higher than the lowest value. The filtered water volume at this station was the same as that of the other tows; thus, the reason for this outlier zooplankton density is unclear. However, we did not remove this extremely low zooplankton density from the GAM analyses.

3.2. Horizontal distributions and body lengths of tuna larvae

A total of 13 539 scombrid larvae were collected during the 3 cruises. While 2796 specimens, including 2025 specimens of *Auxis* spp., were genetically identified using an allele-specific PCR assay, we could not identify 15 specimens to the species level because of PCR errors due to DNA template quantity and/or quality. The identified larvae included some rare species: 3 individuals were identified as *Euthynnus affinis*, and 68, 4, and 1 individuals were identified as bigeye tuna, longtail tuna *Thunnus tonggol*, and albacore *T. alalonga*, respectively, in the 2015 cruise. The last 3 species were not sampled in the other 2 cruises and were only identified morphologically. These minor species and the specimens that were not identified due to DNA errors, damage, or a too-small size were eliminated in all following analyses (0.7% of total scombrid larvae).

PBF, YFT, SKJ, BT, and FT larvae were collected during each cruise. BT was the most dominant species throughout the cruises, with mean densities per cruise of 91.7, 51.6, and 14.7 larvae 1000 m^{-3} in 2015, 2016, and 2017, respectively (Fig. 3, Table 2). In contrast, the mean densities per cruise of FT larvae were only 2.3, 1.6, and 1.9 larvae 1000 m^{-3} in 2015, 2016, and 2017, respectively (Fig. 3, Table 2), and FT was the fifth most dominant species in this area in all years except for 2017. The second, third, and fourth most dominant species were YFT, SKJ, and PBF; notably, the second most dominant species was SKJ in 2015, but SKJ was the fifth most dominant species in 2017. The

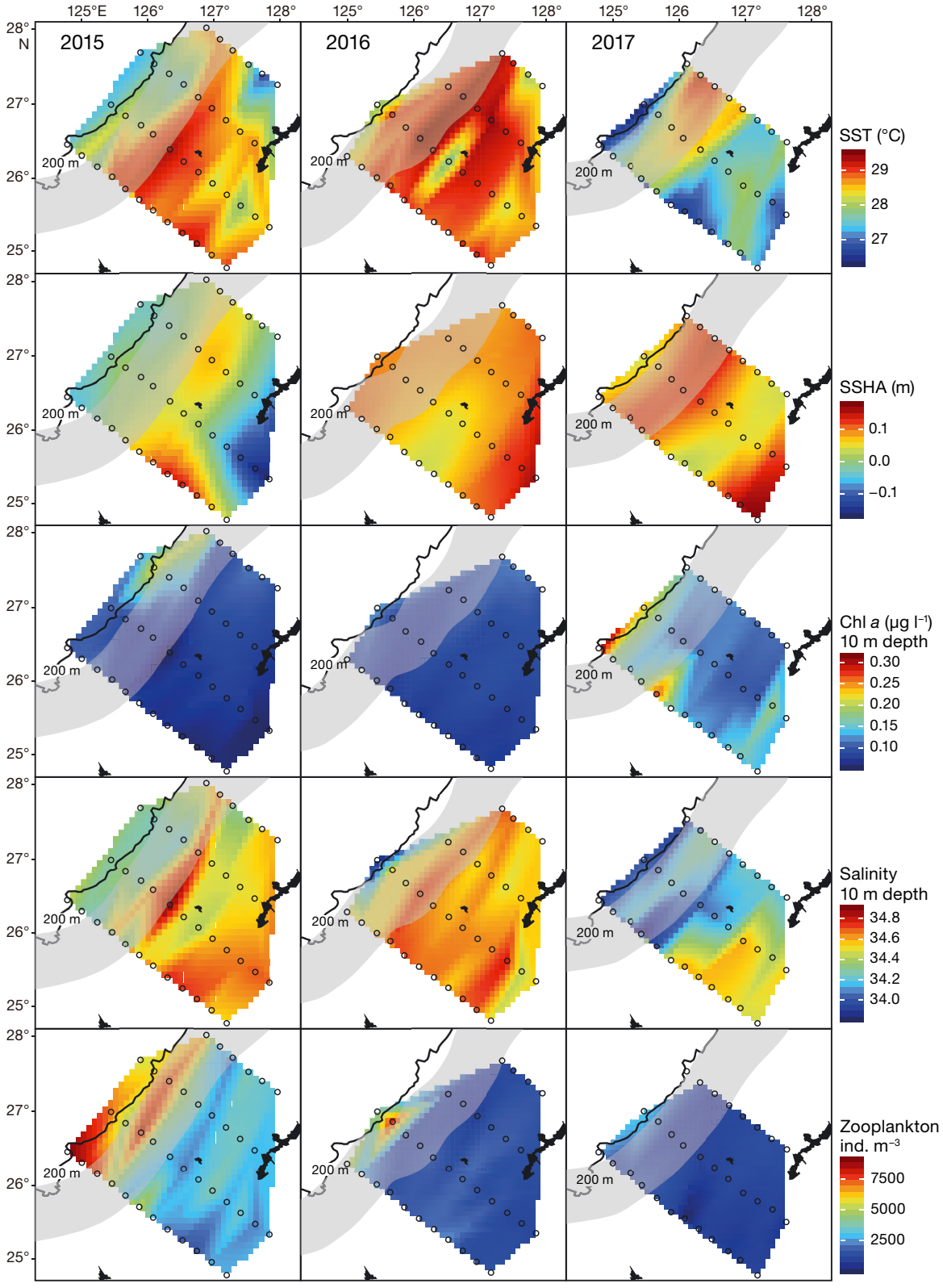

Fig. 2. Inter-annual variability observed for 5 environmental parameters: sea surface temperature (SST), sea surface height anomaly (SSHA), chl *a* concentration at 10 m depth (Chl *a*), salinity at 10 m depth (Salinity), and zooplankton density (Zooplankton) in 2015 (left column), 2016 (center column), and 2017 (right column). The broad grey band indicates the position of the Kuroshio during the observations, open circles show the sampling stations, and the solid line marks the 200 m depth contour

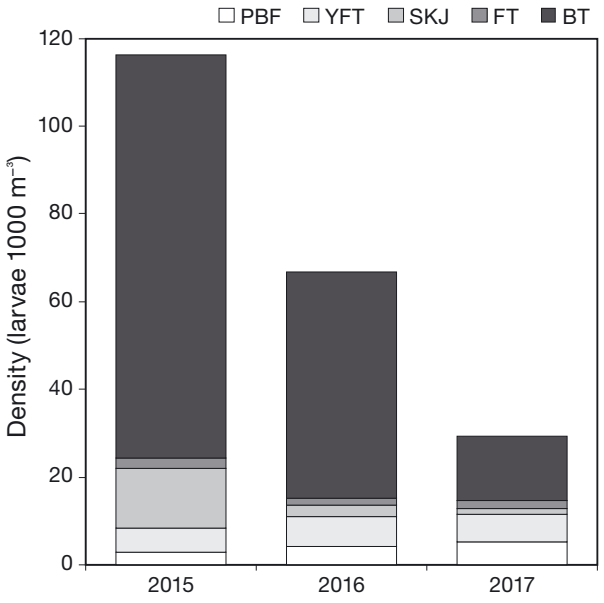

Fig. 3. Density (larvae 1000 m^{-3}) and species composition of larvae of 5 tuna species collected off the Nansei Islands from 2015 to 2017. Species abbreviations as in Table 1

mean densities per cruise of YFT were 5.6, 6.7, and 6.2 larvae 1000 m^{-3} in 2015, 2016, and 2017, respectively, those of PBF were 2.9, 4.3, and 5.3 larvae 1000 m^{-3}, respectively, and those of SKJ were 13.6, 2.6, and 1.4 larvae 1000 m^{-3}, respectively (Fig. 3, Table 2).

The horizontal distributions were clearly different between BT and the other species; BT was mostly collected in the Kuroshio and the Kuroshio inshore waters (Fig. 4). The results of the PCoA showed that BT clustered away from the other 4 tuna species in the combination of the first and second axes (Fig. 5a). The eigenvalues of the first and second axes explained 18.3 and 9.1% of the variation, respectively. According to the first PCoA axis, the positive values of the stations were largely characterized by the dominance of BT, and the stations with high positive values were located at the shelf edge and the Kuroshio (Fig. 5b). The second axis was largely characterized by the dominance of PBF and YFT, which tended to be higher at stations in the Kuroshio offshore waters than in the Kuroshio inshore waters (Fig. 5c).

The mean body lengths of all 5 species of tuna larvae showed interannual variations (Fig. 6); the mean body length of BT was largest in 2016 and significantly smaller in 2015 (Tukey HSD test; $p < 0.001$). The other species showed similar trends: the mean body lengths were smallest in 2015 and largest in 2017. BT larvae were significantly larger than FT larvae in 2015 and 2016 (Tukey HSD test; $p < 0.01$), while BT larvae were smaller than FT larvae in 2017 (Tukey HSD test; $p < 0.05$). There was no significant negative relationship between the larval abundance and mean body length at any station except for SKJ. The mode of PBF body length was 4–5 mm, while the body lengths of YFT, SKJ, FT, and BT were 5–6 mm.

3.3. GAMs

The AIC best-fit models for the 5 dominant species are shown in Table 1. In total, 51.5, 40.6, 53.3, 10.4, and 76.7% of the variance was explained by the final models for PBF, YFT, SKJ, FT, and BT, respectively (Table 1).

The SSHA was selected in all cases, although we observed a positive relationship between SSHA and the abundance of SKJ and a negative relationship between SSHA and the abundance of FT (Fig. 7). Regarding the local maximum responses of PBT, YFT, and BT, the effect was negative when SSHA was >0.1 m high for PBF and YFT, while for BT, the local maximum was observed between –0.05 and 0 m (Fig. 7).

The distance from the Kuroshio (Dist) was also selected in all cases except for YFT (Fig. 7). The local maximum responses of PBF and SKJ to Dist were observed at 50–100 and 20–50 n miles away from the Kuroshio northern edge, respectively. On the other hand, negative relationships were observed for FT

Table 2. Number of larvae and larval density (ind. 1000 m^{-3}) of 5 tuna species collected off the Nansei Islands from 2015 to 2017. Species abbreviations as in Table 1

Year	Stations	PBF		YFT		SKJ		FT		BT	
	(n)	n	Density	n	Density	n	Density	n	Density	n	Density
2015	39	220	2.9	404	5.6	947	13.6	171	2.3	6474	91.7
2016	33	235	4.3	364	6.7	140	2.6	89	1.6	2912	51.6
2017	31	263	5.3	305	6.2	66	1.4	101	1.9	757	14.7
Total	103	718		1073		1153		361		10143	
Average			4.2		6.2		5.9		1.9		52.7

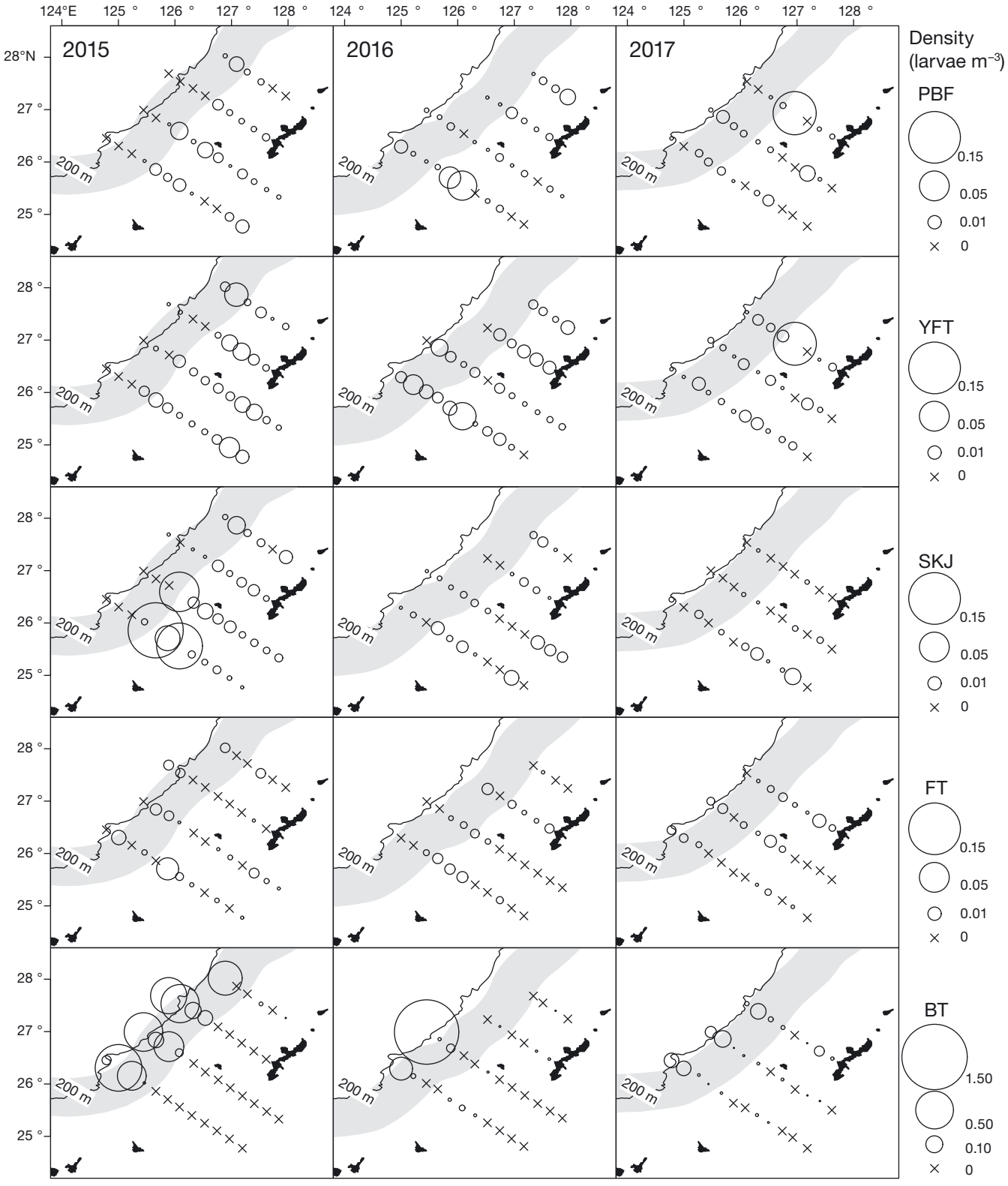

Fig. 4. Horizontal distributions of the densities of 5 species of larval tuna in 2015 (left column), 2016 (center column), and 2017 (right column). Circles indicate presence, and different sizes reflect density (larvae 1000 m^{-3}). Crosses indicate absence of individuals at a sampled station. The broad grey band indicates the Kuroshio, and the solid line shows the 200 m depth contour. The scale for bullet tuna is 10 times larger than for the other species, indicating large differences in larval densities observed. Species abbreviations as in Table 1

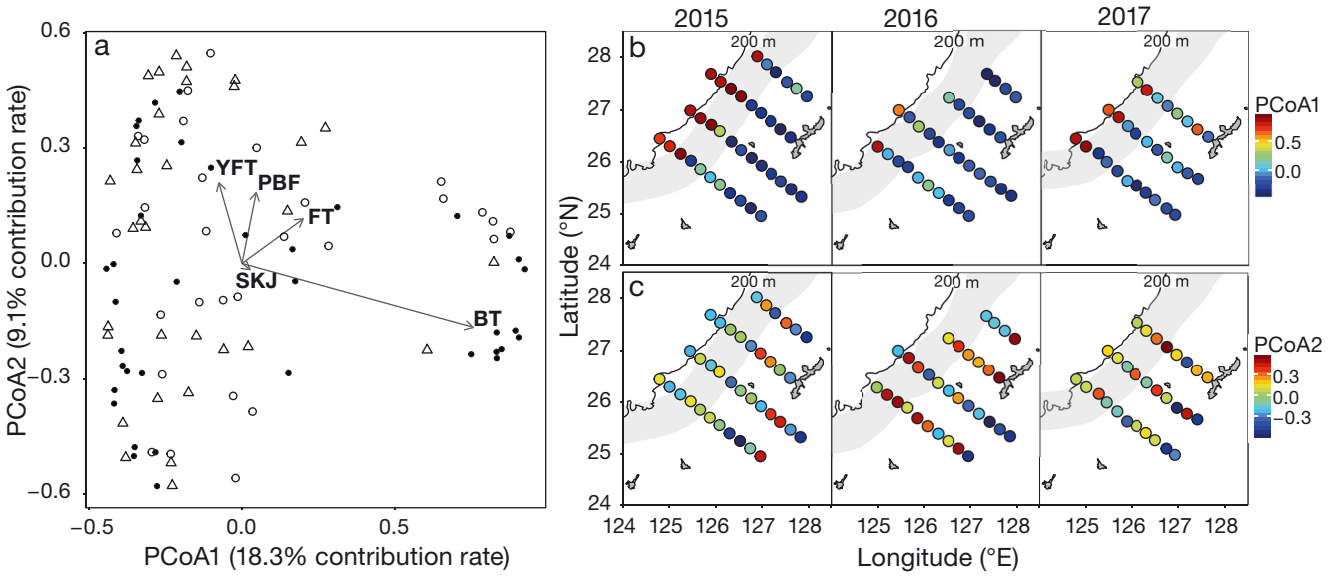

Fig. 5. (a) Principal coordinate analysis (PCoA) biplots of the first and second axes and (b,c) distribution map for each year with projected scores for (b) the first axis and (c) the second axis for species composition at each station. Vector plots of the 5 species used in the PCoA are overlaid (arrows). Symbols show the sampling stations during the 2015 (●), 2016 (△), and 2017 (○) cruises. In (b) and (c), the broad grey band indicates the Kuroshio Current. Species abbreviations as in Table 1

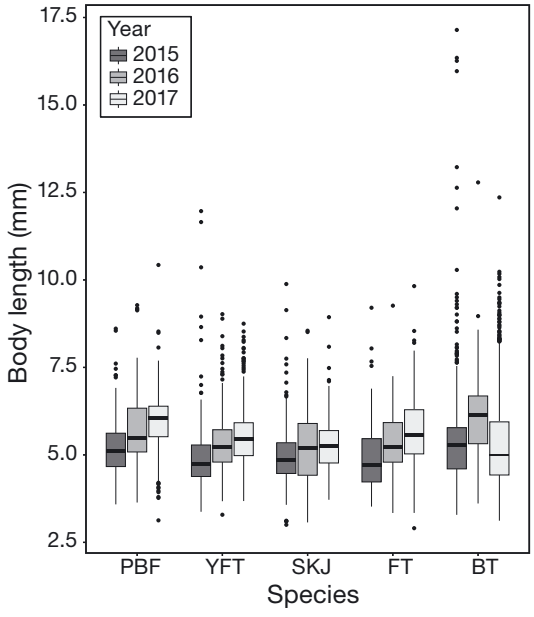

Fig. 6. Body lengths (mm) of larvae of the 5 tuna species collected off the Nansei Islands from 2015 to 2017. Solid symbols indicate outliers. Species abbreviations as in Table 1. Each box shows the interquartile range, and the bold line within each box indicates the median. The whiskers (solid line) extend to the nearest value within 1.5 times interquartile range

and BT larvae. The BD was associated with the YFT and SKJ densities; a shallow BD had positive effects on both species.

SST and salinity at S10, which may be associated with larval physiology, were selected as explanatory parameters for all tunas except FT (Fig. 7). SST was selected for PBF and YFT, and salinity was selected for YFT, SKJ, and BT. The local maximum response to SST was observed in the range of 28.5–29°C for both PBF and YFT, and negative effects were observed in water <28°C. A positive relationship with salinity was observed for YFT and SKJ, and a negative relationship with salinity was observed for BT. BT was the only tuna associated with zooplankton density, for which a positive relationship was observed. The effect of year was selected in all cases except FT; the trend was similar to that of the mean abundance of each species.

4. DISCUSSION

This study is the first quantitative evaluation of the habitats of multiple species of tuna larvae off the coast of the Nansei area across the Kuroshio. The larvae collected in our study were considered to be a critical size (approximately 5 mm body length) because survival of PBF larvae hatch in Nansei waters depends largely on their growth rate in this size class (Watai et al. 2017, 2018, Ishihara et al. 2019). Although the recruitment processes of the other species in this area were not reported, the most important period for tuna species larvae is 1 or 2 wk after hatching; therefore, the evaluation of the habitats of tuna and tuna-like species in our study is important not only for larval ecology but also for recruitment of tunas.

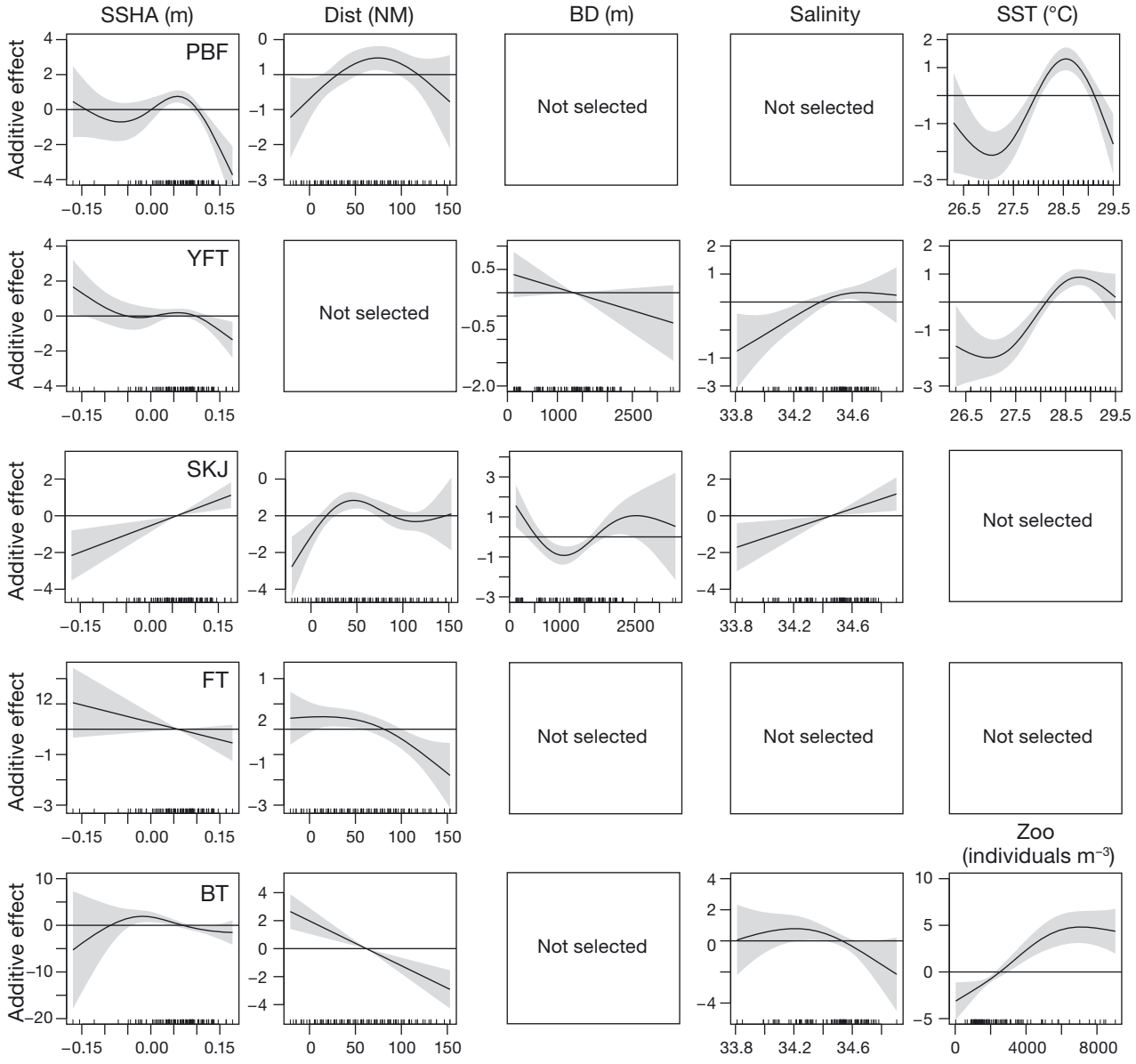

Fig. 7. Smoothing functions for all explanatory variables from the optimal generalized additive model selected based on the lowest value of Akaike's information criterion, including the offset [log(volume)]. The grey band indicates the 95% confidence interval. SSHA: sea surface height anomaly (m); Dist: distance from the northern edge of the Kuroshio (n miles); BD: bottom depth (m); Salinity: salinity at 10 m depth; SST: sea surface temperature (°C); Zoo: zooplankton density (ind. m^{-3}). Species abbreviations as in Table 1

We consistently observed 5 tuna species (PBF, YFT, SKJ, FT, and BT) in samples collected off the coast of the Nansei Islands during the PBF spawning season. These results suggest that overlaps among the ecological niches of the 5 species should be considered with respect to Gause's competitive exclusion principle, which posits that multiple species inhabiting the same niche cannot stably co-exist (Hardin 1960).

Before discussing the relationship between oceanic environments and the density of larvae, we must consider the effects of larval size on larval density, which was not addressed in our GAMs. In general, larval abundance decreases exponentially with growth (Anderson 1988). In our study, however, a clear decreasing tendency between mean larval size and abundance was not observed in any tuna species except SKJ. In addition, although the mesh size of our gear was small enough (0.334 mm) to sample small larvae (<3 mm), the mode of the larval body length was 4–6 mm long. Therefore, we considered the lar-

val densities at every station to indicate whether the environments were suitable for survival of spawners and larvae and whether eggs/larvae amassed at the station (i.e. larval densities reflected survival rates, initial egg densities, and passive transport).

Initially, our observation area was largely influenced by the Kuroshio, and the fine-scale horizontal distributions of the 5 dominant species were grouped into 2 categories corresponding to the Kuroshio based on the GAM analysis: BT and FT larvae were dominant in the Kuroshio and the Kuroshio inshore waters, and SKJ and PBF larvae were dominant in the Kuroshio offshore waters (>40 n miles away from the northern edge). BT larvae were more common in the Kuroshio inshore waters than FT larvae, and PBF larvae more common in the Kuroshio offshore waters then SKJ larvae. According to the GAM, the distribution of YFT was not characterized by the Kuroshio, but was limited to Kuroshio offshore waters, similar to SKJ and PBF (Fig. 4). Our results were consistent with previous studies on the distributions of larvae and eggs in this area (Suzuki et al. 2014, Sassa & Konishi 2015, Lin et al. 2016); larvae and eggs of BT and FT have been found in the East China Sea inside the Kuroshio (Sassa & Konishi 2015, Lin et al. 2016), and larval PBF patches have been found off the coast of the Nansei Islands outside of the Kuroshio (Suzuki et al. 2014). The distributions of SKJ and YFT larvae represent the first information on these species in this area since the study by Nishikawa et al. (1985) 3 decades ago.

Oceanic currents, including eddies, have an impact on larval distributions because they accumulate and diffuse larvae (Bakun 1996, 2006, 2013). The horizontal distribution of larval tunas is also associated with the ocean currents in the Gulf of Mexico and the Mediterranean Sea (Mariani et al. 2010, Lindo-Atichati et al. 2012, Domingues et al. 2016). However, the variations in larval distributions in the Kuroshio area were not considered to be the result of accumulation; the current velocity (>2 knots) of the Kuroshio is too high for larvae to stay in our observation area, and the Kuroshio reaches not only the south of Honshu (the mainland of Japan) but also the central part of the North Pacific as the Kuroshio Extension.

We considered whether the different responses to the Kuroshio among tuna larvae were the result of differences in spawning areas. PBF spawners are caught in the Kuroshio offshore waters (Chen et al. 2006, Shimose et al. 2018), and YFT fisheries have historically occurred in the Kuroshio offshore waters (Suzuki et al. 1978). BT and FT are considered coastal species (Matsuura & Sato 1981, Sabatés & Recasens 2001) that are abundant in the coastal area of the East China Sea and Taiwan Strait (Tao et al. 2012), and BT eggs are collected during summer on the shelf of the East China Sea (Lin et al. 2016). BD may be a variable that explains spawning area, but BD only explained the distributions of YFT and SKJ larvae in this study because larval tunas are not distributed at depths >100 m. The distributions of adults in the spawning season corresponded with the larval distribution found in our present study; however, the spawning grounds of these tuna species might change annually at a fine scale.

Meso-scale eddies evidently influence the larval distributions; in general, warm core anticyclonic eddies (the high SSHA values) physically aggregate plankton (Bakun 1996, 2006, 2013). Thus, if the larval horizontal distributions are controlled by passive transport, all of the studied larvae, particularly the 3 species in the Kuroshio offshore waters, should have been observed in high-SSHA waters. The response of larvae to the SSHA in the GAM showed that the larval SKJ clearly amassed in the warm core eddies, but the other 2 species accumulated only moderately. Therefore, the relationship between SSHA and larval density indicated that the larval distribution was controlled not only by passive transport but also by oceanographic conditions that affect larval physiology and survival, i.e. SST, salinity, and zooplankton densities.

SST had an effect on 2 species of *Thunnus* larvae. SST has been used as an index of larval tuna habitats in previous studies on PBF (Ohshimo et al. 2017, Muhling et al. 2018). Ohshimo et al. (2017) showed that PBF larvae usually occur at SSTs ranging from 24–29°C, and this range is wider than that in our study; in particular, the lower limit of our study (28.2°C) is high. Different from Ohshimo et al. (2017), our observation period was limited to June, and the GAMs of our present study showed that the distribution of PBF was limited not only by SST but also by the distance from the Kuroshio and by SSHA. In particular, the distance from the Kuroshio limited the optimal temperature range of PBF because low SST waters were observed only in the Kuroshio inshore waters, where PBF larvae were not found. The temperature response patterns in the GAMs were similar between PBF and YFT, while the optimal SST for YFT was slightly higher than that for PBF. The positive response range of PBF to temperature in the GAMs was within the optimal temperature range of rearing experiments (Miyashita & Sudo 2005), but that of YFT to temperature was higher than the optimal temperature range (23–26°C) of rearing experiments for hatching and normal growth (Kim et al. 2015).

The salinity at 10 m depth was also selected as an explanatory variable for the abundance of YFT, SKJ, and BT. Based on the GAMs, positive correlations between the abundances of 2 species (YFT and SKJ) and salinity were observed; however, there was a negative correlation between BT and salinity. Rearing experiments have indicated that saline water is suitable for YFT hatching and normal growth (Kim et al. 2015), which supports our results. Cornic et al. (2018) indicated that larval YFT can adapt to a wide range of salinity in the Gulf of Mexico, and Lang et al. (1994) reported that the highest growth of YFT was observed in less-saline (salinity 31) waters of that area. We believe that the high growth and dominance of YFT in the less-saline waters of the Gulf of Mexico is supported by the high productivity of this region due to nutrient inputs from the Mississippi River, as discussed by Cornic et al. (2018). In the Kuroshio offshore waters, the contributions of riverine input to salinity are negligible (Kodama et al. 2011), and thus, the response of YFT larvae to salinity differs between the Nansei area and the Gulf of Mexico.

The density of BT was positively associated with zooplankton density. Considering that the BT larvae were distributed in the Kuroshio inshore waters, they likely adapted to more eutrophic conditions than larvae of the other 4 tuna species. In contrast to the BT larval density, the other larval densities were not associated with zooplankton density. In a previous study, the food condition was important for larval growth and survival of PBF (Satoh et al. 2013) and southern bluefin tuna *T. maccoyii* (Jenkins et al. 1991). Therefore, the larval density was expected to be associated with the zooplankton densities, but this was not the case. In the Gulf of Mexico, the abundance of Atlantic bluefin tuna was positively associated with high zooplankton densities (Muhling et al. 2010).

We have 2 hypotheses explaining why the total zooplankton only explained the BT larval density and not the densities of the other 4 species: (1) larval tunas are highly selective zooplankton feeders; thus, total zooplankton density cannot be used as a food condition index; (2) there was a mismatch in the vertical distributions of larvae and zooplankton or between sampling time and feeding time. Regarding the first hypothesis, larval PBF in the Sea of Japan are reported to be selective feeders (Kodama et al. 2017), and during the study period, we confirmed that larval PBF preyed on Cladocera based on morphological identification; Cladocera are rarely observed in the water column (Kodama et al. in press). These results indicate that PBF larvae are selective feeders in both the Nansei area and the Sea of Japan. A global comparative study indicated that diet compositions are different among co-occurring species of larval tunas and concluded that larval tunas are highly selective feeders (Llopiz & Hobday 2015); the diet compositions of different tunas should thus differ in the studied area. Therefore, total zooplankton density may not be a suitable index of food conditions. Regarding the second hypothesis, the zooplankton density in 0–20 m was positively related to that in 0–200 m, but this relationship was not strong ($r^2 = 0.3$). Globally, larval tunas are mainly present in surface waters (Habtes et al. 2014, Reglero et al. 2018), which includes the PBF in the Nansei area (Satoh 2010). In addition, our observations were conducted at night when larval tuna could not feed and zooplankton migrated to the shallow layer.

Horizontal overlaps of larval tuna habitats were observed. One overlap was between the 2 *Auxis* species, and the other was among SKJ, YFT, and PBF. This study is the first quantitative assessment of the larval habitats of these 2 *Auxis* species. Lin et al. (2016) identified eggs to the species level using genetic techniques, but the larval habitats were not determined. In other previous studies, the habitats of *Auxis* spp. were not divided into 2 species (Boehlert & Mundy 1994), or only 1 species (BT) was identified in the survey area (Morote et al. 2008). Notably, although tuna distributions overlapped in our study, the fine-scale distributions were different; the first axis of PCoA showed that when BT was dominant, the FT density was low (Fig. 5). The GAM results indicated that the density of larval BT was high in the productive and less-saline water. Therefore, between these 2 species, BT larvae may be at a disadvantage under oligotrophic conditions compared to FT larvae.

In the Kuroshio offshore waters, the horizontal distributions of SKJ, YFT, and PBF larvae were not clearly separated. On the basis of Gause's competitive exclusion principle (Hardin 1960), differences in other habitats, such as vertical distributions and feeding habits, must be considered. In the Nansei area, no studies have investigated the vertical distributions and feeding habits of multiple species of larval tunas. However, regarding the vertical distributions of tunas, larval SKJ show significant diel migrations (Richards & Simmons 1971, Matsumoto et al. 1984, Davis et al. 1990, Boehlert & Mundy 1994), whereas PBF larvae stay within the surface layer at depths ≤20 m, with no significant diel migrations (Satoh 2010). The segregation of main prey items has also been observed in co-occurring larval tunas (Llopiz & Hobday 2015). These differences may ex-

plain the co-occurrence and survival of larval tunas in the Nansei area because the co-occurrence of juvenile tunas has also been observed in our survey area (Chow et al. 2003).

5. CONCLUSIONS

We evaluated the horizontal segregation of larvae of 5 tuna species and evaluated the environmental factors of the habitats of these species off the Nansei Islands for the first time. Over the 3 yr study, we consistently observed 5 tuna species belonging to 3 genera (*Thunnus*, *Katsuwonus*, and *Auxis*) in our samples. BT larvae were dominant throughout the observations, whereas the second to fifth most dominant species differed in each sampling year. The horizontal distributions of the 5 species were influenced by the Kuroshio: the 2 *Auxis* species were mainly distributed in the Kuroshio and the Kuroshio inshore waters, and the other 3 species were distributed in the Kuroshio offshore waters. The distributions of the 2 larval *Auxis* species overlapped, but a high density of larval BT was observed in zooplankton-rich, less-saline waters, while the larval FT density was not explained by these parameters. Larval distributions of SKJ, YFT, and PBF also overlapped in the Kuroshio offshore waters. The environmental parameters (temperature, salinity, SSHA) explained the distributions of these 3 species; however, the responses of these 3 species to environmental parameters were similar.

Considering Gause's competitive exclusion principle, to maintain the species richness of larval tunas in the Kuroshio offshore waters, the other habitats of the larval tunas, particularly those of SKJ, YFT, and PBF, are expected to be different. Vertical distributions and feeding habits are also expected to differ among species, but in the Nansei area, evaluations of vertical distributions and feeding habits have not been conducted for any tuna except for PBF. Therefore, future research should evaluate the larval tuna habits in the Nansei area to better understand the recruitment processes of tunas.

Acknowledgements. We are grateful to the captains, officers, and crews of the RV 'Shunyo-Maru' for their field assistance. We thank Drs. K. Nohara and H. Takeshima, Tokai University, for their assistance with species identification, and M. Okazaki, National Research Institute of Far Seas Fishery (NRIFSF), for assistance with the acquisition of satellite data. We also thank members of the Bluefin Tuna Biology Laboratory, NRIFSF, for assistance with sample measurement and AVISO for providing the SSHA data. This study was financially supported by the Japan Fisheries Agency.

LITERATURE CITED

Anderson JT (1988) A review of size dependent survival during pre-recruit stages of fishes in relation to recruitment. J Northwest Atl Fish Sci 8:55–66

Ashida H, Suzuki N, Tanabe T, Suzuki N, Aonuma Y (2015) Reproductive condition, batch fecundity, and spawning fraction of large Pacific bluefin tuna *Thunnus orientalis* landed at Ishigaki Island, Okinawa, Japan. Environ Biol Fishes 98:1173–1183

Bakun A (1996) Patterns in the ocean: ocean processes and marine population dynamics, Vol 61. California Sea Grant, in cooperation with Centro de Investigaciones Biologicas del Noroeste, La Paz

Bakun A (2006) Fronts and eddies as key structures in the habitat of marine fish larvae: opportunity, adaptive response and competitive advantage. Sci Mar 70: 105–122

Bakun A (2013) Ocean eddies, predator pits and bluefin tuna: implications of an inferred 'low risk–limited payoff' reproductive scheme of a (former) archetypical top predator. Fish Fish 14:424–438

Boehlert GW, Mundy BC (1994) Vertical and onshore-offshore distributional patterns of tuna larvae in relation to physical habitat features. Mar Ecol Prog Ser 107:1–13

Chen KS, Crone P, Hsu CC (2006) Reproductive biology of female Pacific bluefin tuna *Thunnus orientalis* from south-western North Pacific Ocean. Fish Sci 72:985–994

Chow S, Nohara K, Tanabe T, Itoh T and others (2003) Genetic and morphological identification of larval and small juvenile tunas (Pisces: Scombridae) caught by a mid-water trawl in the western Pacific. Suisan Sougou Kenkyuu Senta Kenkyuu Houkoku 8:1–14

Collette BB, Carpenter KE, Polidoro BA, Juan-Jorda MJ and others (2011) High value and long life — double jeopardy for tunas and billfishes. Science 333:291–292

Cornic M, Smith BL, Kitchens LL, Alvarado Bremer JR, Rooker JR (2018) Abundance and habitat associations of tuna larvae in the surface water of the Gulf of Mexico. Hydrobiologia 806:29–46

Davis TLO, Jenkins GP, Young JW (1990) Diel patterns of vertical distribution in larvae of southern bluefin *Thunnus maccoyii*, and other tuna in the East Indian Ocean. Mar Ecol Prog Ser 59:63–74

Domingues R, Goni G, Bringas F, Muhling B, Lindo Atichati D, Walter J (2016) Variability of preferred environmental conditions for Atlantic bluefin tuna (*Thunnus thynnus*) larvae in the Gulf of Mexico during 1993–2011. Fish Oceanogr 25:320–336

Gower JC (1967) Multivariate analysis and multidimensional geometry. Statistician 17:13–28

Habtes S, Muller-Karger FE, Roffer MA, Lamkin JT, Muhling BA (2014) A comparison of sampling methods for larvae of medium and large epipelagic fish species during spring SEAMAP ichthyoplankton surveys in the Gulf of Mexico. Limnol Oceanogr Methods 12:86–101

Hardin G (1960) The competitive exclusion principle. Science 131:1292–1297

Houde E (1997) Patterns and trends in larval stage growth and mortality of teleost fish. J Fish Biol 51:52–83

Ishihara T, Watai M, Ohshimo S, Abe O (2019) Differences in larval growth of Pacific bluefin tuna (*Thunnus orientalis*) between two spawning areas, and an evaluation of the growth-dependent mortality hypothesis. Environ Biol Fishes 102:581–594

Jenkins GP, Young JW, Davis TLO (1991) Density dependence of larval growth of a marine fish, the Southern bluefin tuna, *Thunnus maccoyii.* Can J Fish Aquat Sci 48: 1358–1363

Kawai H (1969) Statistical estimation of isotherms indicative of the Kuroshio axis. Deep Sea Res 16:109–115

Kim YS, Delgado DI, Cano IA, Sawada Y (2015) Effect of temperature and salinity on hatching and larval survival of yellowfin tuna *Thunnus albacares*. Fish Sci 81: 891–897

Kodama T, Furuya K, Hashihama F, Takeda S, Kanda J (2011) Occurrence of rain-origin nitrate patches at the nutrient-depleted surface in the East China Sea and the Philippine Sea during summer. J Geophys Res 116:C08003

Kodama T, Setou T, Masujima M, Okazaki M, Ichikawa T (2015) Intrusions of excess nitrate in the Kuroshio subsurface layer. Cont Shelf Res 110:191–200

Kodama T, Hirai J, Tamura S, Takahashi T and others (2017) Diet composition and feeding habits of larval Pacific bluefin tuna *Thunnus orientalis* in the Sea of Japan: integrated morphological and metagenetic analysis. Mar Ecol Prog Ser 583:211–226

Kodama T, Hirai J, Tawa A, Ishihara T, Ohshimo S (2020) Feeding habits of the Pacific Bluefin tuna (*Thunnus orientalis*) larvae in two nursery grounds based on morphological and metagenomic analyses. Deep Sea Res II (in press) doi:10.1016/j.dsr2.2020.104745

Lang KL, Grimes CB, Shaw RF (1994) Variations in the age and growth of yellowfin tuna larvae, *Thunnus albacares*, collected about the Mississippi River plume. Environ Biol Fishes 39:259–270

Legendre P, Legendre L (2012) Numerical ecology, Vol 24. Elsevier, Amsterdam

Leggett WC, Deblois E (1994) Recruitment in marine fishes: Is it regulated by starvation and predation in the egg and larval stages? Neth J Sea Res 32:119–134

Lin HY, Chiu MY, Shih YM, Chen IS, Lee MA, Shao KT (2016) Species composition and assemblages of ichthyoplankton during summer in the East China Sea. Cont Shelf Res 126:64–78

Lindo-Atichati D, Bringas F, Goni G, Muhling B, Muller-Karger FE, Habtes S (2012) Varying mesoscale structures influence larval fish distribution in the northern Gulf of Mexico. Mar Ecol Prog Ser 463:245–257

Llopiz JK, Hobday AJ (2015) A global comparative analysis of the feeding dynamics and environmental conditions of larval tunas, mackerels, and billfishes. Deep Sea Res II 113:113–124

Majkowski J (2007) Global fishery resources of tuna and tuna-like species. Fish Tech Pap 483. FAO, Rome

Mariani P, MacKenzie BR, Iudicone D, Bozec A (2010) Modelling retention and dispersion mechanisms of bluefin tuna eggs and larvae in the northwest Mediterranean Sea. Prog Oceanogr 86:45–58

Matsumoto WM, Skillman RA, Dizon AE (1984) Synopsis of biological data on skipjack tuna, *Katsuwonus pelamis.* NOAA Tech Rep NMFS Circ 451. https://repository.library.noaa.gov/view/noaa/5555

Matsuura Y, Sato G (1981) Distribution and abundance of scombrid larvae in southern Brazilian waters. Bull Mar Sci 31:824–832

Miyashita S, Sudo M (2005) Effects of water temperature and salinity on the mortality at the early stage. Annual Reports on 21st century COE program. Kinki University (in Japanese)

Morote E, Olivar MP, Pankhurst PM, Villate F, Uriarte I (2008) Trophic ecology of bullet tuna *Auxis rochei* larvae and ontogeny of feeding-related organs. Mar Ecol Prog Ser 353:243–254

Muhling BA, Lamkin JT, Roffer MA (2010) Predicting the occurrence of Atlantic bluefin tuna (*Thunnus thynnus*) larvae in the northern Gulf of Mexico: building a classification model from archival data. Fish Oceanogr 19: 526–539

Muhling BA, Tommasi D, Ohshimo S, Alexander MA, DiNardo G (2018) Regional-scale surface temperature variability allows prediction of Pacific bluefin tuna recruitment. ICES J Mar Sci 75:1341–1352

Nakayama SI, Fukuda H, Nakatsuka S (2019) Model-free time series analysis detected the contributions of middle-age spawner biomass and the environment on Pacific bluefin tuna recruitment. ICES J Mar Sci (in press) doi: 10.1093/icesjms/fsz129

Nishikawa Y, Honma M, Ueyanagi S, Kikawa S (1985) Average distribution of larvae of oceanic species of scombroid fishes, 1956–1981. Far Seas Fish Res Lab 12:1–99

Ohshimo S, Tawa A, Ota T, Nishimoto S and others (2017) Horizontal distribution and habitat of Pacific bluefin tuna, *Thunnus orientalis*, larvae in the waters around Japan. Bull Mar Sci 93:769–787

Ohshimo S, Sato T, Okochi Y, Ishihara Y and others (2018a) Long-term change in reproductive condition and evaluation of maternal effects in Pacific bluefin tuna, *Thunnus orientalis*, in the Sea of Japan. Fish Res 204:390–401

Ohshimo S, Sato T, Okochi Y, Tanaka S, Ishihara T, Ashida H, Suzuki N (2018b) Evidence of spawning among Pacific bluefin tuna, *Thunnus orientalis*, in the Kuroshio and Kuroshio-Oyashio transition area. Aquat Living Resour 31:33

Okiyama M (2014) An atlas of early stage fishes in Japan. Tokai University Press, Kanagawa

Okochi Y, Abe O, Tanaka S, Ishihara Y, Shimizu A (2016) Reproductive biology of female Pacific bluefin tuna, *Thunnus orientalis*, in the Sea of Japan. Fish Res 174: 30–39

Oksanen J, Blanchet FG, Friendly M, Kindt R and others (2019) 'vegan': Community ecology package. R package version 2.5-6. https://cran.r-project.org/package=vegan

Core Team (2018) R: a language and environment for statistical computing. R Foundation for Statistical Computing, Vienna

Reglero P, Tittensor DP, Alvarez-Berastegui D, Aparicio-Gonzalez A, Worm B (2014) Worldwide distributions of tuna larvae: revisiting hypotheses on environmental requirements for spawning habitats. Mar Ecol Prog Ser 501:207–224

Reglero P, Blanco E, Alemany F, Ferra C and others (2018) Vertical distribution of Atlantic bluefin tuna *Thunnus thynnus* and bonito *Sarda sarda* larvae is related to temperature preference. Mar Ecol Prog Ser 594:231–243

Richards WJ, Simmons DC (1971) Distribution of tuna larvae (Pisces, Scombridae) in the northwestern Gulf of Guinea and off Sierra Leone. Fish Bull 69:555–568

Sabatés A, Recasens L (2001) Seasonal distribution and spawning of small tunas (*Auxis rochei* and *Sarda sarda*) in the Northwestern Mediterranean. Sci Mar 65:95–100

Sassa C, Konishi Y (2015) Late winter larval fish assemblage in the southern East China Sea, with emphasis on spatial relations between mesopelagic and commercial pelagic fish larvae. Cont Shelf Res 108:97–111

Satoh K (2010) Horizontal and vertical distribution of larvae of Pacific bluefin tuna *Thunnus orientalis* in patches entrained in mesoscale eddies. Mar Ecol Prog Ser 404: 227–240

Satoh K, Tanaka Y, Masujima M, Okazaki M, Kato Y, Shono H, Suzuki K (2013) Relationship between the growth and survival of larval Pacific bluefin tuna, *Thunnus orientalis*. Mar Biol 160:691–702

Shimose T, Aonuma Y, Tanabe T, Suzuki N, Kanaiwa M (2018) Solar and lunar influences on the spawning activity of Pacific bluefin tuna (*Thunnus orientalis*) in the south-western North Pacific spawning ground. Fish Oceanogr 27:76–84

Suzuki Z, Tomlinson PK, Honma M (1978) Population structure of Pacific yellowfin tuna. Inter-Am Trop Tuna Comm Bull 17:274–441

Suzuki N, Tanabe T, Nohara K, Doi W, Ashida H, Kameda T, Aonuma Y (2014) Annual fluctuation in Pacific bluefin tuna (*Thunnus orientalis*) larval catch from 2007 to 2010 in waters surrounding the Ryukyu Archipelago, Japan. Suisan Sougou Kenkyuu Senta Kenkyuu Houkoku 38:87–99

Tanaka Y, Satoh K, Iwahashi M, Yamada H (2006) Growth-dependent recruitment of Pacific bluefin tuna *Thunnus orientalis* in the northwestern Pacific Ocean. Mar Ecol Prog Ser 319:225–235

Tanaka Y, Tawa A, Ishihara T, Sawai E, Nakae M, Masujima M, Kodama T (2020) Occurrence of Pacific bluefin tuna *Thunnus orientalis* larvae off the Pacific coast of Tohoku area, northeastern Japan: possibility of the discovery of the third spawning ground. Fish Oceanogr 29:46–51

Tao Y, Mingru C, Jianguo D, Zhenbin L, Shengyun Y (2012) Age and growth changes and population dynamics of the black pomfret (*Parastromateus niger*) and the frigate tuna (*Auxis thazard thazard*), in the Taiwan Strait. Lat Am J Aquat Res 40:649–656

Watai M, Ishihara T, Abe O, Ohshimo S, Strussmann CA (2017) Evaluation of growth-dependent survival during early stages of Pacific bluefin tuna using otolith microstructure analysis. Mar Freshw Res 68:2008–2017

Watai M, Hiraoka Y, Ishihara T, Yamasaki I, Ota T, Ohshimo S, Strüssmann CA (2018) Comparative analysis of the early growth history of Pacific bluefin tuna *Thunnus orientalis* from different spawning grounds. Mar Ecol Prog Ser 607:207–220

Welschmeyer NA (1994) Fluorometric analysis of chlorophyll-*a* in the presence of chlorophyll-*b* and pheopigments. Limnol Oceanogr 39:1985–1992

Wood SN (2017) Generalized additive models: an introduction with R. CRC Press, Boca Raton, FL

Editorial responsibility: Myron Peck, Hamburg, Germany

Submitted: March 8, 2019; Accepted: December 12, 2019
Proofs received from author(s): February 6, 2020